AIAA JOURNAL
Vol. 36, No. 5, May 1998

Evaluation of Layerwise Mixed Theories for Laminated Plates Analysis

Erasmo Carrera*
Turin Polytechnic Institute, Turin 10129, Italy

The evaluation of mixed layerwise theories to calculate the in-plane and out-of-plane responses of thick plates in two-dimensional modeling of multilayered structures is made. The employed models, which were proposed by the author in earlier works, a priori fulfill the continuity of transverse shear and normal stress components at the interface between two adjacent layers. A Reissner's mixed variational equation is used to derive the governing equations, in terms of introduced stress and displacement variables. The interface continuity conditions are imposed by writing the governing equations at a multilayered level. The related standard displacement formulations are also discussed for comparison purpose. Closed-form solutions are presented for plates made of orthotropic lamina and bent by harmonic distribution of transverse pressure. Symmetrically and unsymmetrically laminated, as well as sandwich, plates have been investigated. A comparison with a three-dimensional-elasticity analysis shows that present mixed layerwise models furnish a better description of the in-plane and out-of-plane response of thick plates with respect to existing layerwise and equivalent single-layer theories. In particular, the proposed models describe, with excellent accuracy, the transverse shear and normal stress fields. Unlike available current models, these fields are herein determined a priori without requiring implementation of any postprocessing procedures. The distribution of the transverse displacement and transverse normal stress in the plate thickness direction are also shown for most of the problems.

I. Introduction

THE evaluations of transverse shear and normal stress and the related effects have played an important, constant role in thick-multilayered-plate analyses. Recent interest in such evaluations is due to the use of composite materials in primary thick components. In fact, as laminated materials undergo transition from secondary to primary structural components, the goals of analysis must be broadened to include the highly accurate assessment of localized regions where damage is likely to take place. As experienced by early three-dimensional elasticity analyses,[1–3] the variation of the mechanical properties in the thickness direction of laminated structures, for compatibility and equilibrium reasons, leads to displacement and transverse stress fields, which reveal discontinuous derivatives in correspondence to each interface. The so-called zigzag form of displacement fields and interlaminar continuity for the transverse stresses were summarized in Ref. 4 using the term C_z^0 requirements, that is, displacement and transverse stress fields must be C^0-continuous functions in the plate thickness direction z. Furthermore, the mentioned three-dimensional elasticity analyses underlined the fundamental role played by transverse normal stress. Nevertheless, three-dimensional-elasticity solutions are available in only a few cases, which are mainly related to simple geometries, specific stacking sequence of the lamina, and linear problems. In the most general cases and to minimize the computational effort, two-dimensional models are preferred in practice. In this respect, an enormous number of models and approximated techniques has been proposed over the last three decades. Exhaustive overviews on these topics can be found in many published review papers. Among these are Refs. 4–8. A short review, which is useful for the purpose of this work, is here given.

Classical models, i.e., classical lamination theories (CLTs) and first-order shear deformation theory (FSDT), have been extended to laminated structures.[9] Higher-order expansions were applied to laminated plates by Lo et al.[10] These theories are based on the displacement formulation and belong to the group of equivalent single-layer models (ESLMs). These models preserve the independence of the number of the independent variables from the numbers of the layers. Unfortunately, CLT and FSDT, as well the model in Ref. 10, do not account for the C_z^0 requirements. Nevertheless, transverse shear stress can be evaluated at a postprocessing level through integration of the three-dimensional indefinite equilibrium equations. The obtained results have, however, shown high inaccuracy in thick plate cases.[1] On the other hand, this postprocessing operation cannot be implemented in the general case of a nonsymmetric in-plane stress response with respect to the plate middle surface,[11] as is in the case for nonlinear analysis.[12]

Improvements, with respect to classical approaches, were achieved through partial fulfillment of the C_z^0 requirements using higher-order shear deformation theories (HSDTs). A pioneering analysis was presented by Yu,[13] where in-plane zigzag effects and transverse shear continuity were both fulfilled in correspondence to the two interfaces of a sandwich plate. Zero top–bottom plate conditions on the transverse shear stress were implemented to laminated structures by Reddy.[14] Cho and Parmerter[15] included in-plane zigzag effects and transverse shear continuity for arbitrarily laminated plates in a five-degree-of-freedom model. This work could be considered the best version of displacement-based theories that have originated from Refs. 16–18. Among HSDT models, particular mention should be made of the excellent work by Ren.[19] Ren extended very early work by Lekhnitstkii[20,21] to anisotropic plates that had originally been presented for multilayered beams. In contrast to Ref. 15, zigzag kinematics were not assumed by Ren but were derived by means of a stress function formulation. The resulting seven-degree-of-freedom model (two more than the one by Cho and Parmerter[15]) a priori fulfilled the three-dimensional indefinite equilibrium equations, showing excellent agreement with respect to three-dimensional elasticity solutions.

Unfortunately, because of the intrinsic material couplings between the transverse normal and in-plane stress components, all of the mentioned ESLMs experienced difficulties in extending the zigzag forms to the transverse displacement component or in accounting for the interlaminar continuity of the transverse normal stress. As a consequence, all of the related results have shown deficiencies in analyzing problems in which transverse normal stress plays a determinant role.[11,22] The present paper does not overview results and theories based on the method of asymptotic

Received April 15, 1997; revision received Dec. 19, 1997; accepted for publication Dec. 23, 1997.

*Research Professor, Department of Aeronautics and Aerospace Engineering, Corso Duca degli Abruzzi, 24. E-mail: carrera@polito.it. Member AIAA.

expansion.[23,24] In particular one can refer to the recent work by Hodges et al.[25] and Satyrin and Hodges,[26] where an optimum Reissner-like theory, based on asymptotic correction, is presented.

Better results were obtained by employing models in which two-dimensional approximations were introduced at a layer level: layerwise models (LWMs). The number of the unknown variables remains dependent on the number of layers.[27,28] From a computational point of view, LWMs are more expensive than ESLM. The local–global strategies[11,29] have also been proposed to minimize computational efforts: LWMs are used in those regions of the structures in which an accurate description is required, whereas ESLMs are employed in the remaining parts. However, LWM results have shown acceptable accuracy with respect to three-dimensional analyses, but available models do not a priori and completely fulfill C_z^0 requirements. LWMs based on displacement formulation cannot normally account for a priori transverse stress interlaminar continuity. In fact, transverse stresses are generally evaluated a posteriori via integration of three-dimensional indefinite equilibrium equations.

In these scenarios, the convenience of assuming two independent fields for displacement and transverse stress components appeared evident to Reissner.[30,31] As a result, he proposed a mixed equation as a tool to variationally establish governing equilibrium and constitutive equations in terms of the introduced displacement and stress variables. This mixed equation has been used by Murakami,[32] Toledano and Murakami,[33,34] Rao and Meyer-Piening,[35] and Carrera[36] in the field of ESLM formulation. Even though Refs. 34 and 35 a priori and completely included the C_z^0 requirements, the obtained results have shown a high deficiency in treating arbitrarily laminated plates. In those cases in which an accurate description is required, the use of a mixed equation, therefore, requires a layerwise description. Toledano and Murakami, who in Ref. 33 employed Reissner's mixed equation to propose a layerwise theory, also knew of this conclusion. Unfortunately, in Ref. 33 the transverse normal stress has been discarded, and consequently, the model has resulted in severe limitations to analyze very thick structures.

From the preceding discussion, the following conclusions emerge. 1) ESLMs can undergo difficulties in analyzing very thick, multilayered plates; in particular, they lead to a poor description of the transverse normal stress and related consequences. In this respect, the use of LWM is required. 2) Reissner's mixed approaches furnish the possibility of a priori and completely introducing the C_z^0 requirements. 3) Transverse normal stress cannot be neglected in thick plates analysis.

The author has shown the convenience of referring to the Reissner mixed variational equations in multilayered plate analysis in view of the fulfillment of the C_z^0 requirements in a recent series of papers based on these conclusions.[4,22,37] In Ref. 4, mixed ESLMs and LWMs were proposed. Attention was focused on approximated solution techniques, and the resulting governing equations were written as a system of algebraic equations. A weak form of Hooke's law was also introduced into this work to reduce the mixed cases to the displacement ones. Further discussions and subcase theories were provided in Ref. 22, where finite element applications were outlined. The strong form of the layerwise theories was provided in a subsequent paper by deriving the governing differential equations in terms of stress and strain resultants.[37] A standard displacement formulation was also used in Ref. 37 for comparison. A few numerical results, restricted to cross-ply, symmetrically laminated thick plates, showed the accuracy of the mixed models in the a priori evaluation of transverse normal stress fields. Such accuracy encouraged the further analyses and discussion reported in the present work.

The paper has been organized as follows. The material and geometrical models, as well as the assumed displacement and transverse stress layerwise fields, are described in the next section. The governing equations related to both displacements and mixed formulations are given in Sec. III in terms of the introduced variables. With respect to Ref. 37, the governing equations at a layer level in terms of stress and displacement variables are herein explicitly given in Appendices A–C. C_z^0 requirements are imposed in Sec. IV, where assembly from a layer to a multilayered level is described. A closed-form solution of a Navier type is also discussed in this section for the case of orthotropic lamina. A numerical investigation is presented in Sec. V, where transverse shear and normal stresses are evaluated for thin and thick plates. Symmetric and nonsymmetric laminates, as well as sandwich plates, have been investigated. A comparison with available results is given. The main conclusions are summarized in the last section.

II. Basic Assumptions

The geometry and the coordinate system of the laminated plates of N_l layers are shown in Fig. 1. The integer k, which is extensively used as both subscripts or superscripts, denotes the layer number that starts from the plate bottom, and x and y are the plate middle surface coordinates. Γ^k is the layer boundary on Ω^k: Γ_g^k and Γ_m^k are those parts of Γ^k on which geometrical and mechanical boundary conditions are imposed, respectively. Here, z and z_k are the plate and layer thickness coordinates h and h_k, respectively. Also, $\zeta_k = (2z_k/h_k)$ is the correspondent nondimensioned local plate coordinate; A_k is the k-layer thickness domain.

To completely and a priori fulfill the C_z^0 requirements, an LWM is assumed for both displacement $\boldsymbol{u}^k$ ($\{u_x^k, u_y^k, u_z^k\}$) and transverse stress fields $\boldsymbol{\sigma}_n^k$ ($\{\sigma_{xz}^k, \sigma_{yz}^k, \sigma_{zz}^k\}$). The following N-order expansion has been chosen in the thickness direction of each k-layer:

$$\boldsymbol{u}^k = F_t\boldsymbol{u}_t^k + F_b\boldsymbol{u}_b^k + F_r\boldsymbol{u}_r^k = F_\tau\boldsymbol{u}_\tau^k \qquad \tau = t, b, r \quad (r = 2, 3, \ldots, N)$$
$$\boldsymbol{\sigma}_{nM}^k = F_t\boldsymbol{\sigma}_{nt}^k + F_b\boldsymbol{\sigma}_{nb}^k + F_r\boldsymbol{\sigma}_{nr}^k = F_\tau\boldsymbol{\sigma}_{n\tau}^k \quad k = 1, 2, \ldots, N_l \tag{1}$$

Subscripts n and M are normal (out-of-plane) components of stresses from the assumed model. Boldfaced symbols are arrays. N is a free parameter. Subscripts t and b are values related to the layer top and bottom surfaces, respectively. They consist of the linear part of the expansion. Higher-order distributions in the z direction (parabolic, cubic, etc.) are introduced by the r polynomials. Short forms have been written by means of the τ index; the usual summation convention is intended for this.

The thickness functions $F_\tau(\zeta_k)$ are defined by

$$F_t = \frac{P_0 + P_1}{2}, \qquad F_b = \frac{P_0 - P_1}{2}, \qquad F_r = P_r - P_{r-2}, \quad r = 2, 3, \ldots, N$$

in which $P_j = P_j(\zeta_k)$ is the Legendre polynomial of j order. The chosen functions have the following properties:

$$\zeta_k = \begin{cases} 1 & : \ F_t = 1, \quad F_b = 0, \quad F_r = 0 \\ -1 & : \ F_t = 0, \quad F_b = 1, \quad F_r = 0 \end{cases}$$

The top and bottom values have been used as unknowns. Based on this, the C_z^0 requirements can be easily linked. In fact, the compatibility of the displacement and the equilibrium for the transverse stress components read

$$\boldsymbol{u}_t^k = \boldsymbol{u}_b^{(k+1)}, \qquad k = 1, N_l - 1$$
$$\boldsymbol{\sigma}_{nt}^k = \boldsymbol{\sigma}_{nb}^{(k+1)}, \qquad k = 1, N_l - 1 \tag{2}$$

In those cases in which the top/bottom plate stress values are prescribed (zero or imposed values), the following additional C_z^0-requirements must be accounted for:

$$\boldsymbol{\sigma}_{nb}^1 = \bar{\boldsymbol{\sigma}}_{nb}, \qquad \boldsymbol{\sigma}_{nt}^{N_l} = \bar{\boldsymbol{\sigma}}_{nt} \tag{3}$$

where the overbar is the imposed values in correspondence to the plate top $k = N_l$ and bottom $k = 1$. As one remains within the small deformation field, the in-plane and out-of-plane strain components $\boldsymbol{\epsilon}_p^k$ ($\{\epsilon_{xx}^k, \epsilon_{yy}^k, \epsilon_{xy}^k\}$) and $\boldsymbol{\epsilon}_n^k$ ($\{\epsilon_{xz}^k, \epsilon_{yz}^k, \epsilon_{zz}^k\}$) are linearly related to the displacements $\boldsymbol{u}^k$ according to the following geometrical relations:

$$\boldsymbol{\epsilon}_{pG}^k = \boldsymbol{D}_p\boldsymbol{u}^k, \qquad \boldsymbol{\epsilon}_{nG}^k = \boldsymbol{D}_n\boldsymbol{u}^k \tag{4}$$

The subscript G signifies that the previous strains originate from geometrical relations, whereas $\boldsymbol{D}_p$ and $\boldsymbol{D}_n$ are in-plane and out-of-plane differential operators, respectively (see Appendix A).

The lamina is considered to be homogeneous and to operate in the linear elastic range. By employing stiffness coefficients, Hooke's

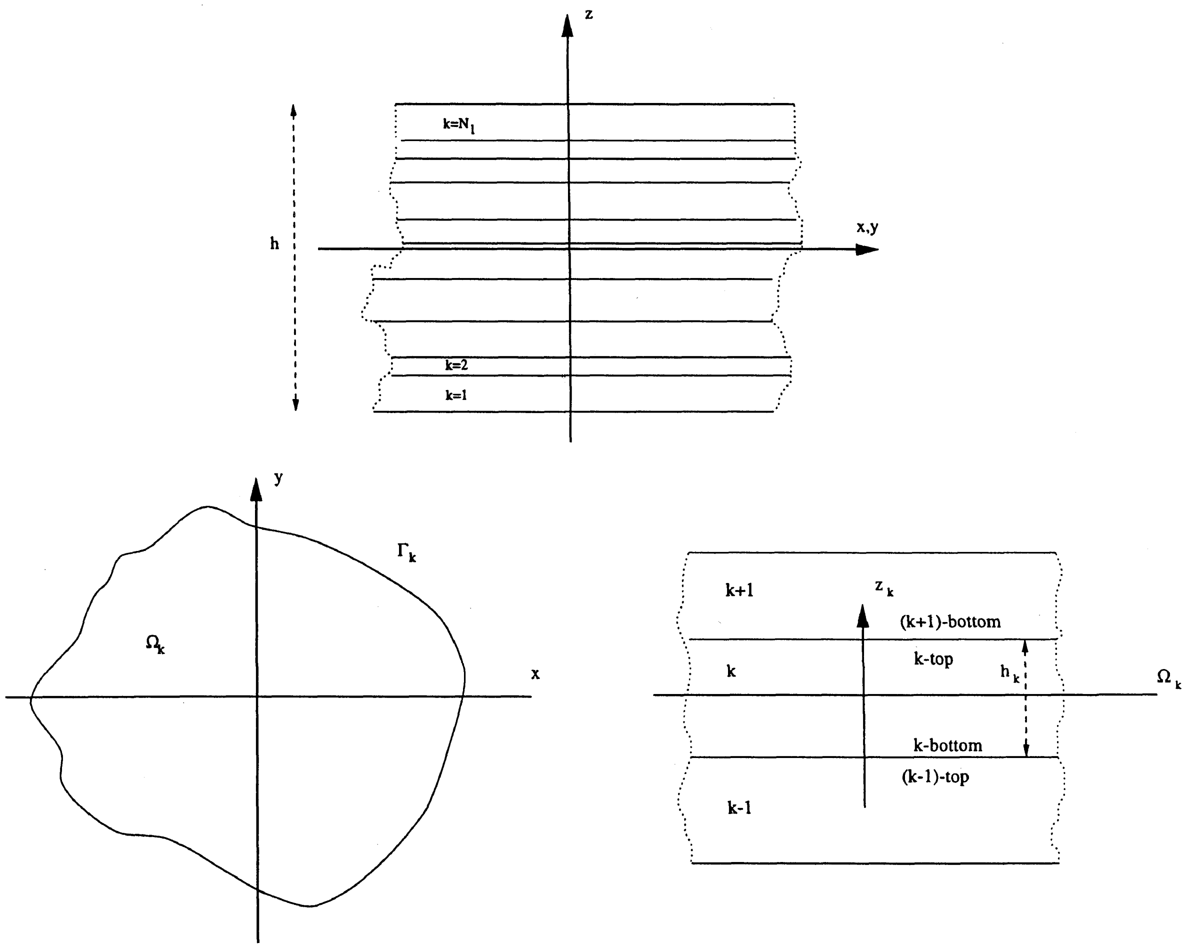

Fig. 1 Geometry and notation of multilayered plates.

law for the anisotropic k lamina is written in the form $\sigma_i = \tilde{C}_{ij}\epsilon_j$, where the indices i and j, ranging from 1 to 6, stand for the index couples 11, 22, 33, 13, 23, and 12, respectively. The material is assumed to be orthotropic, as specified by $\tilde{C}_{14} = \tilde{C}_{24} = \tilde{C}_{34} = \tilde{C}_{64} = \tilde{C}_{15} = \tilde{C}_{25} = \tilde{C}_{35} = \tilde{C}_{65} = 0$. This implies that σ^k_{xz} and σ^k_{yz} depend only on ϵ^k_{xz} and ϵ^k_{yz}. In matrix form,

$$\begin{aligned} \boldsymbol{\sigma}^k_{pH_d} &= \tilde{\boldsymbol{C}}^k_{pp}\boldsymbol{\epsilon}^k_{pG} + \tilde{\boldsymbol{C}}^k_{pn}\boldsymbol{\epsilon}^k_{nG} \\ \boldsymbol{\sigma}^k_{nH_d} &= \tilde{\boldsymbol{C}}^k_{np}\boldsymbol{\epsilon}^k_{pG} + \tilde{\boldsymbol{C}}^k_{nn}\boldsymbol{\epsilon}^k_{nG} \end{aligned} \tag{5}$$

and $\boldsymbol{\sigma}^k_p$ ($\{\sigma^k_{xx}, \sigma^k_{yy}, \sigma^k_{xy}\}$) are the in-plane stress components. Subscripts H are stresses evaluated using Hooke's law, whereas subscript G is the strain obtained from the geometrical relations equation (4). A further subscript d signifies values employed in the displacement formulation. Equation (5) is used in conjunction with a standard displacement formulation, whereas for the adopted mixed solution procedure, the stress–strain relationships are conveniently put in the following mixed form:

$$\begin{aligned} \boldsymbol{\sigma}^k_{pH} &= \boldsymbol{C}^k_{pp}\boldsymbol{\epsilon}^k_{pG} + \boldsymbol{C}^k_{pn}\boldsymbol{\sigma}^k_{nM} \\ \boldsymbol{\epsilon}^k_{nH} &= \boldsymbol{C}^k_{np}\boldsymbol{\epsilon}^k_{pG} + \boldsymbol{C}^k_{nn}\boldsymbol{\sigma}^k_{nM} \end{aligned} \tag{6}$$

where both stiffness and compliance coefficients are employed. The relation between the arrays of coefficients of the two forms of Hooke's law is

$$\boldsymbol{C}^k_{pp} = \tilde{\boldsymbol{C}}^k_{pp} - \tilde{\boldsymbol{C}}^k_{pn}\left(\tilde{\boldsymbol{C}}^k_{nn}\right)^{-1}\tilde{\boldsymbol{C}}^k_{np}, \qquad \boldsymbol{C}^k_{pn} = \tilde{\boldsymbol{C}}^k_{pn}\left(\tilde{\boldsymbol{C}}^k_{nn}\right)^{-1}$$

$$\boldsymbol{C}^k_{np} = -\left(\tilde{\boldsymbol{C}}^k_{nn}\right)^{-1}\tilde{\boldsymbol{C}}^k_{np}, \qquad \boldsymbol{C}^k_{nn} = \left(\tilde{\boldsymbol{C}}^k_{nn}\right)^{-1}$$

Superscript -1 denotes an inversion of arrays. Explicit forms are given in Appendix A.

III. Governing Equations for the Lamina

The displacement approach is formulated in terms of $\boldsymbol{u}^k$ by variationally imposing the equilibrium via the principle of virtual displacements. In the static case this establishes

$$\sum_{k=1}^{N_l}\int_{\Omega^k}\int_{A_k}\left(\delta\boldsymbol{\epsilon}^{k^T}_{pG}\boldsymbol{\sigma}^k_{pH_d} + \delta\boldsymbol{\epsilon}^{k^T}_{nG}\boldsymbol{\sigma}^k_{nH_d}\right)\mathrm{d}\Omega^k\,\mathrm{d}z = \delta L^e \tag{7}$$

where δ are virtual variations, whereas superscript T stands for arrays transposition. The variation of the internal work has been split into in-plane and out-of-plane parts and involves the stress obtained from Hooke's law and the strain from the geometrical relations. Here, δL_e is the virtual variation of the work done by the external layer forces $\boldsymbol{p}^k$ ($\{p^k_x, p^k_y, p^k_z\}$).

In the mixed case, the equilibrium and compatibility are both formulated in terms of the $\boldsymbol{u}^k$ and $\boldsymbol{\sigma}^k_n$ unknowns via Reissner's variational equation[30,31]:

$$\begin{aligned} \sum_{k=1}^{N_l}\int_{\Omega^k}\int_{A_k}&\left[\delta\boldsymbol{\epsilon}^{k^T}_{pG}\boldsymbol{\sigma}^k_{pH} + \delta\boldsymbol{\epsilon}^{k^T}_{nG}\boldsymbol{\sigma}^k_{nM}\right. \\ &\left. + \delta\boldsymbol{\sigma}^{k^T}_{nM}\left(\boldsymbol{\epsilon}^k_{nG} - \boldsymbol{\epsilon}^k_{nH}\right)\right]\mathrm{d}\Omega^k\,\mathrm{d}z = \delta L^e \end{aligned} \tag{8}$$

The left-hand side (LHS) includes the variations of the internal work in the plate: The first two terms come from the displacement formulation; they lead to variationally consistent equilibrium conditions; and the third mixed term variationally enforces the compatibility of the transverse strains components.

On substitution of Eqs. (1) and (4–6) and by integrating by parts, the two earlier variational equations lead to governing differential equations in terms of the introduced stress and displacement variables. The governing equations were written in terms of stress and strain resultants in Ref. 37, where details on the treatment of the variational equations are quoted.

The displacement formulation yields to the following equilibrium conditions:

$$\delta \boldsymbol{u}_\tau^k:\ \boldsymbol{K}_d^{k\tau s}\boldsymbol{u}_s^k = \boldsymbol{p}_\tau^k \tag{9}$$

The related boundary conditions are

$$\boldsymbol{u}_\tau^k = \bar{\boldsymbol{u}}_\tau^k \qquad \text{or} \qquad \boldsymbol{\Pi}_d^{k\tau s}\boldsymbol{u}_s^k = \boldsymbol{\Pi}_d^{k\tau s}\bar{\boldsymbol{u}}_s^k \tag{10}$$

whereas the mixed case leads to the following set of equilibrium and constitutive equations:

$$\begin{aligned} \delta \boldsymbol{u}_\tau^k&:\ \boldsymbol{K}_{uu}^{k\tau s}\boldsymbol{u}_s^k + \boldsymbol{K}_{u\sigma}^{k\tau s}\boldsymbol{\sigma}_{ns}^k = \boldsymbol{p}_\tau^k \\ \delta \boldsymbol{\sigma}_{n\tau}^k&:\ \boldsymbol{K}_{\sigma u}^{k\tau s}\boldsymbol{u}_s^k + \boldsymbol{K}_{\sigma\sigma}^{k\tau s}\boldsymbol{\sigma}_{ns}^k = 0 \end{aligned} \tag{11}$$

and to the boundary conditions

$$\boldsymbol{u}_\tau^k = \bar{\boldsymbol{u}}_\tau^k \qquad \text{or} \qquad \boldsymbol{\Pi}_u^{k\tau s}\boldsymbol{u}_s^k + \boldsymbol{\Pi}_\sigma^{k\tau s}\boldsymbol{\sigma}_{ns}^k = \boldsymbol{\Pi}_u^{k\tau s}\bar{\boldsymbol{u}}_s^k + \boldsymbol{\Pi}_\sigma^{k\tau s}\bar{\boldsymbol{\sigma}}_{ns}^k \tag{12}$$

The subscript/superscript $s = t, b, r$ has been introduced to distinguish the terms related to the introduced variables from those related to their variations. The earlier arrays of differential operators are explicitly written in Appendix B. Their dependence on the arrays introduced in Sec. II is given as

$$\begin{aligned} \boldsymbol{K}_d^{k\tau s} &= -\boldsymbol{D}_p^T\left(\tilde{\boldsymbol{Z}}_{pp}^{k\tau s}\boldsymbol{D}_p + \tilde{\boldsymbol{Z}}_{pn}^{k\tau s}\boldsymbol{D}_{n\Omega} + \tilde{\boldsymbol{Z}}_{pn}^{k\tau s_z}\boldsymbol{D}_{n\Omega}\right) \\ &\quad - \boldsymbol{D}_{n\Omega}^T\left(\tilde{\boldsymbol{Z}}_{np}^{k\tau s}\boldsymbol{D}_p + \tilde{\boldsymbol{Z}}_{nn}^{k\tau s}\boldsymbol{D}_{n\Omega} + \tilde{\boldsymbol{Z}}_{nn}^{k\tau s_z}\right) \\ &\quad + \tilde{\boldsymbol{Z}}_{np}^{k\tau_z s}\boldsymbol{D}_p + \tilde{\boldsymbol{Z}}_{nn}^{k\tau_z s}\boldsymbol{D}_{n\Omega} + \tilde{\boldsymbol{Z}}_{nn}^{k\tau_z s_z} \\ \boldsymbol{\Pi}_d^{k\tau s} &= \boldsymbol{I}_p^T\left(\tilde{\boldsymbol{Z}}_{pp}^{k\tau s}\boldsymbol{D}_p + \tilde{\boldsymbol{Z}}_{pn}^{k\tau s}\boldsymbol{D}_{n\Omega} + \tilde{\boldsymbol{Z}}_{pn}^{k\tau s_z}\boldsymbol{D}_{n\Omega}\right) \\ &\quad + \boldsymbol{I}_{n\Omega}^T\left(\tilde{\boldsymbol{Z}}_{np}^{k\tau s}\boldsymbol{D}_p + \tilde{\boldsymbol{Z}}_{nn}^{k\tau s}\boldsymbol{D}_{n\Omega} + \tilde{\boldsymbol{Z}}_{nn}^{k\tau s_z}\right) \\ \boldsymbol{K}_{uu}^{k\tau s} &= -\boldsymbol{D}_p^T\boldsymbol{Z}_{pp}^{k\tau s}\boldsymbol{D}_p, \qquad \boldsymbol{K}_{u\sigma}^{k\tau s} = -\boldsymbol{D}_p^T\boldsymbol{Z}_{pn}^{k\tau s} + E_{\tau_z s}\boldsymbol{I} - E_{\tau s}\boldsymbol{D}_{n\Omega}^T \\ \boldsymbol{K}_{\sigma u}^{k\tau s} &= E_{\tau s}\boldsymbol{D}_{n\Omega} + E_{\tau s_z}\boldsymbol{I} - \boldsymbol{Z}_{np}^{k\tau s}\boldsymbol{D}_p, \qquad \boldsymbol{K}_{\sigma\sigma}^{k\tau s} = -\boldsymbol{Z}_{nn}^{k\tau s} \\ \boldsymbol{\Pi}_u^{k\tau s} &= \boldsymbol{I}_p^T\boldsymbol{Z}_{pp}^{k\tau s}\boldsymbol{D}_p, \qquad \boldsymbol{\Pi}_\sigma^{k\tau s} = \boldsymbol{Z}_{pn}^{k\tau s} + E_{\tau s}\boldsymbol{I}_{n\Omega}^T \end{aligned} \tag{13}$$

The operators $\boldsymbol{I}$, $\boldsymbol{I}_{n\Omega}$, and $\boldsymbol{I}_p$ are also definite in Appendix A. (The last two arrays come from the integration by parts.[37]) The integration on the thickness coordinate has been a priori carried out as usual in two-dimensional modelings; the following layer stiffnesses and integrals have been introduced:

$$\begin{aligned} &\left(\tilde{\boldsymbol{Z}}_{pp}^{k\tau s}, \tilde{\boldsymbol{Z}}_{pn}^{k\tau s}, \tilde{\boldsymbol{Z}}_{np}^{k\tau s}, \tilde{\boldsymbol{Z}}_{nn}^{k\tau s}, \boldsymbol{Z}_{pp}^{k\tau s}, \boldsymbol{Z}_{pn}^{k\tau s}, \boldsymbol{Z}_{np}^{k\tau s}, \boldsymbol{Z}_{nn}^{k\tau s}\right) \\ &\quad = \left(\tilde{\boldsymbol{C}}_{pp}^{k}, \tilde{\boldsymbol{C}}_{pn}^{k}, \tilde{\boldsymbol{C}}_{np}^{k}, \tilde{\boldsymbol{C}}_{nn}^{k}, \boldsymbol{C}_{pp}^{k}, \boldsymbol{C}_{pn}^{k}, \boldsymbol{C}_{np}^{k}, \boldsymbol{C}_{nn}^{k}\right)E_{\tau s} \\ &\left(\tilde{\boldsymbol{Z}}_{pn}^{k\tau s_z}, \tilde{\boldsymbol{Z}}_{np}^{k\tau_z s}, \tilde{\boldsymbol{Z}}_{nn}^{k\tau s_z}, \tilde{\boldsymbol{Z}}_{nn}^{k\tau_z s}, \tilde{\boldsymbol{Z}}_{nn}^{k\tau_z s_z}\right) \\ &\quad = \left(\tilde{\boldsymbol{C}}_{pn}^{k}E_{\tau s_z}, \tilde{\boldsymbol{C}}_{np}^{k}E_{\tau_z s}, \tilde{\boldsymbol{C}}_{nn}^{k}E_{\tau s_z}, \tilde{\boldsymbol{C}}_{nn}^{k}E_{\tau_z s}, \tilde{\boldsymbol{C}}_{nn}^{k}E_{\tau_z s_z}\right) \\ &\left(E_{\tau s}^k, E_{\tau_z s}, E_{\tau s_z}, E_{\tau_z s_z}^k\right) = \int_{A_k} \left(F_\tau F_s, F_{\tau_z}F_s, F_\tau F_{s_z}, F_{\tau_z}F_{s_z}\right)\mathrm{d}z \end{aligned} \tag{14}$$

Explicit forms of these integrals are given in Appendix C for the two cases of parabolic and linear expansion in Eq. (1). These two cases are treated in the numerical part. Explicit forms of the governing equations for each layer can be written by expanding the introduced subscripts and superscripts in the earlier arrays as follows:

$$k = 1, 2, \ldots, N_l, \qquad \tau = t, r, b, \qquad s = t, r, b \qquad (r = 2, \ldots, N)$$

IV. C_z^0 Requirements and Assembly from Layer to Multilayered Level

The preceding section presented a mixed and standard displacement formulation for the N_l layers that have been considered to be independent. To meet the C_z^0 requirements in Eqs. (2) and (3), a further step must be executed. Such a step becomes natural if one writes the governing equations from a layer to a multilayered level. For instance, one of the k-layer arrays in Eq. (9) or in Eqs. (11) is considered. Such an array is shown in Fig. 2. The nine contributions to this array have been denoted in Fig. 2 by two subscripts related to the top, r variables, and bottom terms. For convenience, these terms are listed in the following order: t, r, b. First, the k-layer arrays are set in a larger, multilayer array by ordering the layer from the plate top $k = N_l$ to the plate bottom $k = 1$. Second the interface conditions in Eqs. (2) are imposed by moving the layer arrays along the diagonal of the multilayer array. As a result one obtains the array drawn in the lower part of Fig. 2. This procedure can be conveniently implemented in a computer code. In fact, such a procedure is similar to standard assembly techniques involved in a finite element implementation.

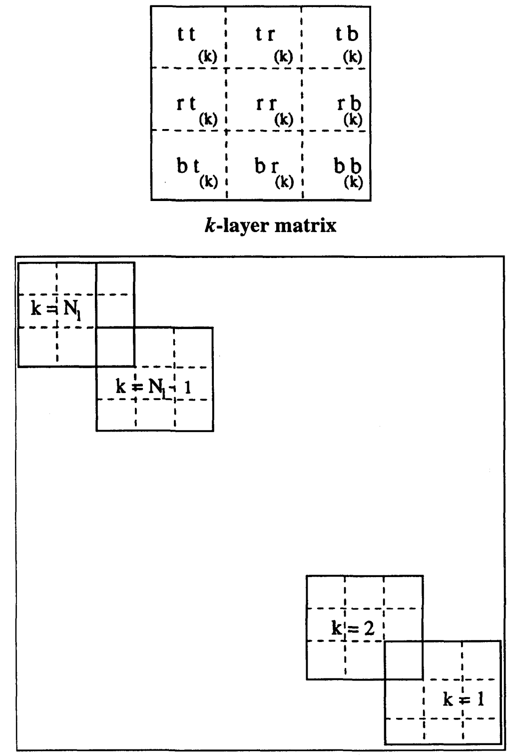

Fig. 2 Assembly of matrices from layers to multilayered level.

The remaining C_z^0 requirements in Eq. (3) can be directly imposed on the multilayer arrays. On multiplication of these arrays for the known top/bottom plate stress values, the dimension of the same arrays and the number of unknown variables are reduced. In the most general case in which a stress or displacement is imposed, such a multiplication produces loading arrays (see subsequent text). After completely imposing the C_z^0 requirements, the arrays of the unknown displacement and stress variables for the whole multilayered plate take on the following forms:

$$\begin{aligned} \boldsymbol{u} &= \left\{\boldsymbol{u}_b^{1^T}, \boldsymbol{u}_t^{1^T}, \boldsymbol{u}_r^{1^T}; \boldsymbol{u}_t^{2^T}, \boldsymbol{u}_r^{2^T}; \ldots; \boldsymbol{u}_t^{k^T}, \boldsymbol{u}_r^{k^T};\right. \\ &\quad \left.\boldsymbol{u}_t^{(k+1)^T}, \boldsymbol{u}_r^{(k+1)^T}; \ldots; \boldsymbol{u}_t^{(N_l-1)^T}, \boldsymbol{u}_r^{(N_l-1)^T}; \boldsymbol{u}_t^{N_l^T}, \boldsymbol{u}_r^{N_l^T}\right\} \\ \boldsymbol{\sigma}_n &= \left\{\boldsymbol{\sigma}_{nt}^{1^T}, \boldsymbol{\sigma}_{nr}^{1^T}; \boldsymbol{\sigma}_{nt}^{2^T}, \boldsymbol{\sigma}_{nr}^{2^T}; \ldots; \boldsymbol{\sigma}_{nt}^{k^T}, \boldsymbol{\sigma}_{nr}^{k^T};\right. \\ &\quad \left.\boldsymbol{\sigma}_{nt}^{(k+1)^T}, \boldsymbol{\sigma}_{nr}^{(k+1)^T}; \ldots; \boldsymbol{\sigma}_{nt}^{(N_l-1)^T}, \boldsymbol{\sigma}_{nr}^{(N_l-1)^T}; \boldsymbol{\sigma}_{nr}^{N_l^T}\right\} \end{aligned} \tag{15}$$

In which the top and the r values have been chosen as layer unknowns.

The governing system of differential equations at a multilayered level for the displacement formulation takes on the following form:

$$\begin{aligned} \boldsymbol{K}_d\boldsymbol{u} = \boldsymbol{p} \qquad &\text{in} \qquad \Omega \\ \boldsymbol{u} = \bar{\boldsymbol{u}} \qquad \text{or} \qquad \boldsymbol{\Pi}_d\boldsymbol{u} = \boldsymbol{\Pi}_d\bar{\boldsymbol{u}} \qquad &\text{on} \qquad \Gamma \end{aligned} \tag{16}$$

whereas for the mixed case, one has

$$\begin{aligned} \boldsymbol{K}_{uu}\boldsymbol{u} + \boldsymbol{K}_{u\sigma}\boldsymbol{\sigma}_n &= \boldsymbol{p} + \boldsymbol{p}_u^{1N_l} \\ \boldsymbol{K}_{\sigma u}\boldsymbol{u} + \boldsymbol{K}_{\sigma\sigma}\sigma_n &= \boldsymbol{p}_\sigma^{1N_l} \end{aligned} \tag{17}$$

with boundary conditions

$$\boldsymbol{u} = \bar{\boldsymbol{u}} \qquad \text{or} \qquad \boldsymbol{\Pi}_u\boldsymbol{u} + \boldsymbol{\Pi}_\sigma\boldsymbol{\sigma}_n = \boldsymbol{\Pi}_u\bar{\boldsymbol{u}} + \boldsymbol{\Pi}_\sigma\bar{\boldsymbol{\sigma}}_n + \boldsymbol{q}_\sigma^{1N_l} \tag{18}$$

where $\boldsymbol{p}_u^{1N_l}, \boldsymbol{p}_\sigma^{1N_l}$, and $\boldsymbol{q}_\sigma^{1N_l}$ are the arrays obtained from the transverse stress values imposed at the top/bottom of the plate in Eq. (3). A more detailed description of the techniques used to build the multilayer arrays is given in Ref. 4.

The boundary values problem governed by Eqs. (16–18) in the most general case of geometry, boundary conditions, and layouts could be solved by implementing only approximated solution procedures. The particular case in which the material has the properties $\tilde{C}_{16} = \tilde{C}_{26} = \tilde{C}_{36} = \tilde{C}_{45} = 0$ has here been considered, for which Navier-type, closed-form solutions can be found by assuming the following harmonic forms for the applied loadings and unknown variables:

$$\begin{aligned} \left(u_{x_\tau}^k, \sigma_{xz_\tau}^k, p_{x_\tau}^k\right) &= \sum_{m,n} \left(U_x^k, S_{xz_\tau}^k, P_{x_\tau}^k\right) \cos\frac{m\pi x}{a} \sin\frac{n\pi y}{b} \\ \left(u_{y_\tau}^k, \sigma_{yz_\tau}^k, p_{y_\tau}^k\right) &= \sum_{m,n} \left(U_y^k, S_{yz_\tau}^k, P_{y_\tau}^k\right) \sin\frac{m\pi x}{a} \cos\frac{n\pi y}{b} \\ \left(u_{z_\tau}^k, \sigma_{zz_\tau}^k, p_{z_\tau}^k\right) &= \sum_{m,n} \left(U_z^k, S_{zz_\tau}^k, P_{z_\tau}^k\right) \sin\frac{m\pi x}{a} \sin\frac{n\pi y}{b} \end{aligned} \tag{19}$$

where a and b are the plate lengths in the x and y directions, respectively, whereas m and n are the correspondent wave numbers. Capital letters on the LHS are correspondent maximum amplitudes. On substitution of Eqs. (19), the governing equations assume the form of a linear system of algebraic equations. The explicit forms assumed by the k-layer arrays are given in Appendix D. Naturally, related multilayer arrays are obtained by implementing the same assemblage just described. This procedure has been coded, and the results are discussed in the next section.

V. Results

In this section the proposed LWM is applied to sample plate problems and compared to available ESLM, LWM, and three-dimensional elasticity solutions. The simply supported plate is bent by a transverse bisinusoidal distribution of normal pressure applied on the top surface of the whole plate $p_{z_t}^{N_l}$. Two problems are discussed: 1) cylindrical bending in the x direction ($m = 1$ and $n = 0$) and 2) square plates ($m = n = 1$). Symmetrically and unsymmetrically laminated, as well as sandwich thick and thin, plates are investigated. In-plane and out-of-plane stress and displacements results are discussed. If not differently declared, the following mechanical data of the lamina are used[1]: $E_L = 25 \times 10^6$ psi, $E_T = 1 \times 10^6$ psi, $G_{LT} = 0.5 \times 10^6$ psi, $G_{TT} = 0.2 \times 10^6$ psi, and $\nu_{LT} = \nu_{TT} = 0.25$, where, following the usual notation,[38] L is the fiber direction, T the transverse direction, and ν_{LT} the major Poisson ratio. The material is assumed to be square-symmetric, and consistent units are referred to. Values corresponding to the plate point in which the stresses and displacements assume their maximum amplitudes in Eq. (19) are quoted in the subsequent analyses. All figures show the distribution of these amplitudes (as ordinate) vs the plate thickness direction z/h (as abscissa).

For comparison purposes, the one-dimensional case related to cylindrical bending treated in Refs. 1, 15, and 33 has first been considered in Table 1 and Figs. 3–6. Table 1 compares the maximum values of the transverse deflection of the midplane for symmetrically and unsymmetrically laminated cylindrically bended thick plates with $a/h = 4$. The maximum traverse displacement is $U_z \times 100 E_T h^3 / P_{z_t}^{N_l} a^4$. Cross-ply (with equal thickness in each layer) and arbitrary laminates described in Tables 2 and 3 are considered. Results related to the present and various other available models are compared to the elasticity solution.[1] The following remarks can be made. Even though transverse normal stress

Table 1 Comparison of present analyses to three-dimensional elasticity and others ESLM and LWM results

Models	$N_l = 3$ 0/90/0	$N_l = 5$ 0/90/0/90/0	$N_l = 4$ 0/90/0/90	$N_l = 3$ Laminated of Table 2	$N_l = 5$ Laminated of Table 2
Elasticity[1]	2.887	3.044	4.181	2.341	2.456
ESLM3[10]	——	——	3.587	——	——
ESLM2[28]	2.907	3.018	3.316	1.992	1.261
ESLM1[15]	——	——	4.083	2.200	2.249
LWM[29]	2.907	3.059	4.202	2.364	2.467
			Present analyses		
M-p	2.891	3.043	4.181	2.341	2.450
	(3.026)	(3.173)	(4.316)	(2.467)	(2.585)
M-1	2.791	3.005	4.163	2.301	2.455
	(2.920)	(3.137)	(4.291)	(2.436)	(2.588)
D-p	2.870	3.040	4.164	2.333	2.443
	(2.999)	(3.171)	(4.282)	(2.463)	(2.578)
D-l	2.783	2.984	4.058	2.304	3.395
	(2.907)	(3.116)	(4.172)	(2.424)	(2.527)

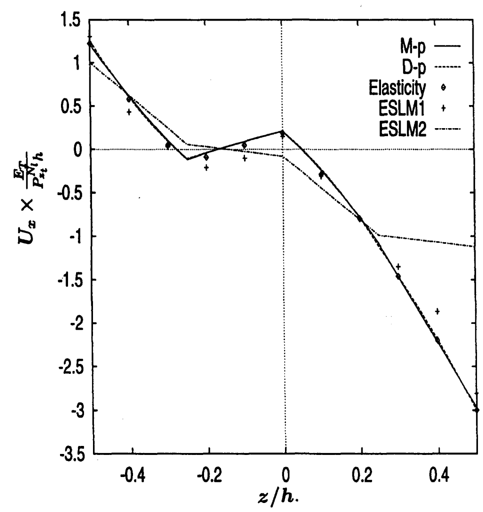

Fig. 3 Amplitude of in-plane displacement $U_x \times (E_T/P_{z_t}^{N_l} h)$ vs z/h; comparison of present and other ESLM results to three-dimensional elasticity[1]; antisymmetric four-layer case, a/h = 4.

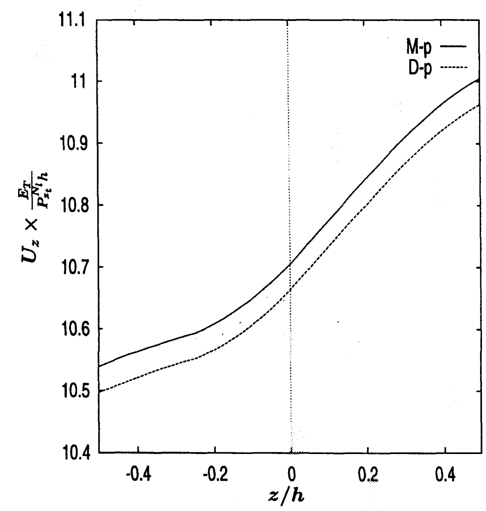

Fig. 4 Amplitude of transverse displacement $U_z \times (E_T/P_{z_t}^{N_l} h)$ vs z/h; comparison between mixed and displacement results; antisymmetric four-layer case, a/h = 4.

is included in ESLM3[10] analysis, better results are obtained by ESLM1,[15] in which such a stress is discarded. Such an improvement must be due to the fact that the C_z^0 requirements are partially fulfilled by the ESLM1 analysis. The model ESLM2[15] (which does not fulfill zero top–bottom plate conditions on the transverse shear stress) consists, in the linear case, of the cubic displacement model ESLM1. Naturally, ESLM1 works better than ESLM2. This becomes much more evident for asymmetrically

Table 2 Geometry of arbitrary three- and five-layer laminates

N_l	k layer	h_k	Material
3	1	0.25	3
	2	0.40	1
	3	0.35	2
5	1	0.10	1
	2	0.25	2
	3	0.15	3
	4	0.20	1
	5	0.30	3

Table 3 Mechanical properties of laminates

Material	$\bar{C}_{11}/E_T$	$\bar{C}_{44}/E_T$
1	1.0025	0.2
2	32.631	8.21
3	25.0627	0.5

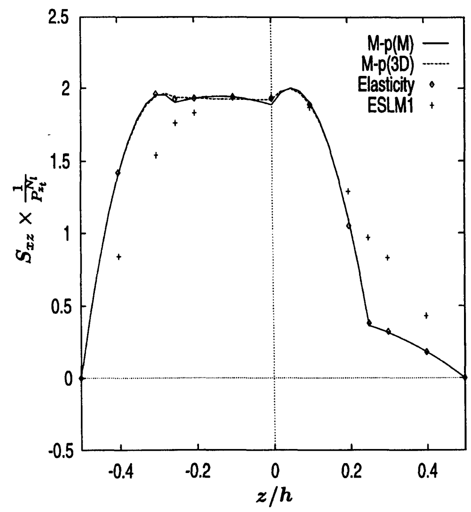

Fig. 5 Transverse shear stress amplitude $S_{xz} \times (1/P_{z_t}^{N_l})$ vs z/h; comparison of present and other ESLM to elasticity[1]; antisymmetric four-layer case, a/h = 4.

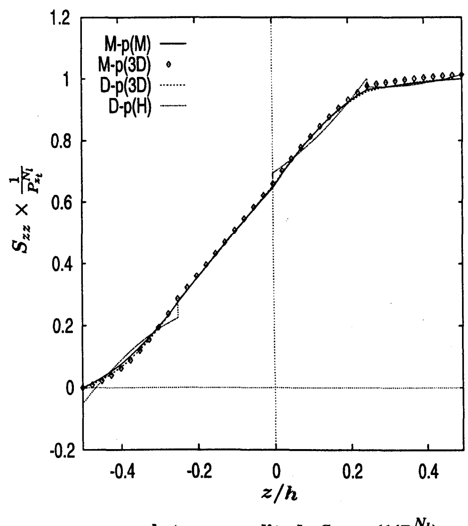

Fig. 6 Transverse normal stress amplitude $S_{zz} \times (1/P_{z_t}^{N_l})$ vs z/h; comparison of different manners of evaluating it; antisymmetric four-layer case, a/h = 4.

laminated plates. Nevertheless, the results obtained using equivalent single-layer theories show a poorer description with respect to the layerwise mixed model in Ref. 33. In this last work the transverse normal stress is neglected, and the transverse shear stress is assumed to be parabolic in each layer, whereas the in-plane displacement field remains linear. The better description obtained in Ref. 33 shows the superiority of LWM results with respect to ESLM analyses. Results related to the present mixed M and displacement D formulations are given in the lower part of Table 1. The present analysis incorporates both a linear l and a parabolic p displacement and/or transverse stress fields in each layer. The transverse displacement being variable in the thickness direction (see also Figs. 4 and 7), the maximum values corresponding to the plate top have been written in parentheses. First, one can notice that, from among the several theories, the present M-p results remain the best description of laminated plates with respect to three-dimensional elasticity. Such accuracy is not affected by stacking sequences of the layers for all of the considered layerwise results: A good description has been obtained for both symmetrically and nonsymmetrically laminated plates.

Figures 3–6 consider the cross-ply, four-layer asymmetrically laminated plates with $a/h = 4$. The distribution of the displacements and transverse shear and normal stresses in the thickness direction have been plotted. Comparisons to three-dimensional elasticity and ESLM results have been presented where available. (Because of the sign of the applied loadings, the signs of the results of other authors have been changed.) Figure 3 confirms what was found in the Table 1 discussion. Figure 4 shows that the thickness variation of the transverse diplacement can be significant. Because of the low average of the transverse anisotropy of the considered multilayered plates, the zigzag effects are barely evident. Figure 5 compares the transverse shear stresses a priori evaluated using the model (M) to those obtained a posteriori by means of integration of the three-dimensional elasticity (3D) indefinite equilibrium equations. The elasticity results quoted in Ref. 15 are also drawn. What has been found in Ref. 37 for symmetrically laminated cases can be extended to arbitrary laminated plates, that is, (M-p) analysis leads to excellent a priori descriptions of the transverse stress fields. Such a priori accuracy cannot be acquired using the ESLM analysis. Figure 6 shows the transverse normal stress field. As underlined in Ref. 29, this stress component has been seldom considered in previous studies. Displacement and mixed results are compared. For the mixed case the value obtained from the model (M) Eq. 1 and those (3D) obtained by postprocessing the three-dimensional indefinite equilibrium equations are given. These last values (3D) and those from Hooke's law Eq. (6) (H) are also plotted for the displacement formulation case. Inescapable numerical errors involved in the postprocessing calculations prohibit an exact fulfillment of the top-plate conditions for both (3D) cases. Furthermore, the use of material law leads to discontinuous stress values in correspondence to the layer interfaces.

A square plate with five layers (cross-ply [0/90/0/90/0] laminated) with equal thickness has been investigated in Figs. 7 and 8 as another problem. Several values of the transverse anisotropy ratio $R_0 = \bar{C}_{ij}^0/\bar{C}_{ij}^{90}$ ($\bar{C}_{ij}^0$ and $\bar{C}_{ij}^{90}$ signify material coefficients of layers whose orientation corresponds to 0 and 90 deg, respectively) and

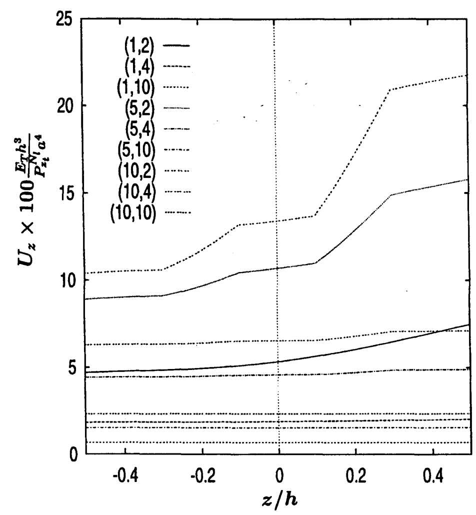

Fig. 7 Transverse normal displacement amplitude $U_z \times 100(E_T h^3/P_{z_t}^{N_l} a^4)$ vs z/h; symmetric cross-ply laminated square plates with different values of transverse anisotropy and thickness ratio (R_0, a/h).

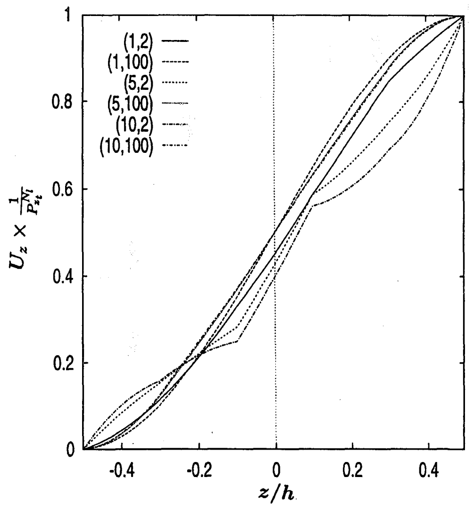

Fig. 8 Transverse normal stress amplitude $U_z \times (1/P_{z_t}^{N_l})$ vs z/h; symmetric cross-ply laminated square plates with different values of transverse anisotropy and thickness ratio (R_0, a/h).

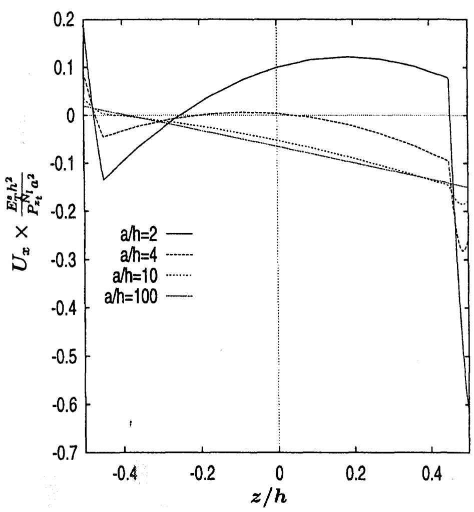

Fig. 9 In-plane displacement amplitude $U_x \times (E_{T_s} h^2/P_{z_t}^{N_l} a^2)$ vs z/h of sandwich plates.

of the thickness ratio a/h have been treated. These values are labeled in parentheses and separated by a comma. An increase in the transverse anisotropy and thickness leads to higher discontinuity of the interface derivatives for both transverse displacement and stress components. It has been confirmed that the variation of u_3 along z cannot be neglected for thick transversely anisotropic plates. As far as transverse normal stresses are concerned, due to the top–bottom plate conditions, it can be remarked that their absolute values do not change very much from thin to thick plates, although it is well known that other stress components increase in thin plates (see also subsequent figures). This is why σ_{zz} can be discarded in thin plate analysis.

The in-plane and out-of-plane characteristics of sandwich thick and thin plates are considered in Figs. 9–12 as a last application. The sandwich consists of an asymmetrically cross-ply [0/0/90] laminated plate. The core coincides to the middle layer. The value of the ratio $R_c = 10$ is considered ($R_0 = \tilde{C}^s_{ij}/\tilde{C}^c_{ij}$, where $\tilde{C}^s_{ij}$ and $\tilde{C}^s_{ij}$ signify material coefficients of skins and core, respectively). The used thickness values of the core and skins are $h_c = 0.9h$ and $h_s = 0.05h$, respectively. The zigzag form of the displacement fields of thick sandwich plates is evident in Figs. 9 and 10. Thick plates show high variations of u_3 in the thickness direction. In-plane normal stress and transverse shear stress values are plotted at Figs. 11 and 12, respectively. The transverse shear deformation capability of skins should not be neglected in thick sandwich cases.

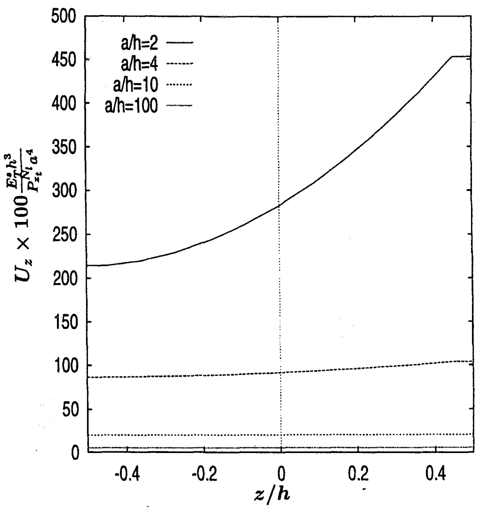

Fig. 10 Transverse displacement $U_z \times 100(E^s_T h^3/P_{z_t}^{N_l} a^4)$ vs z/h of sandwich plates.

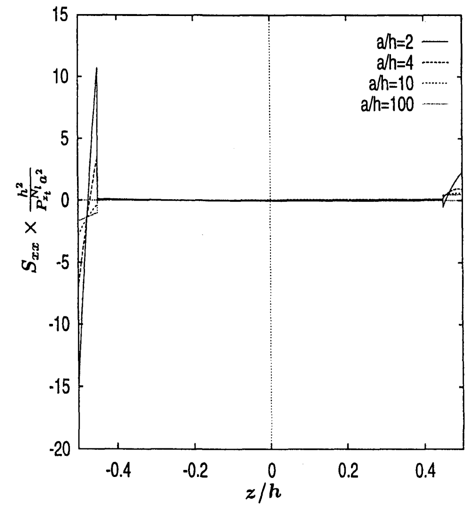

Fig. 11 In-plane stress $S_{xx} \times (h^2/P_{z_t}^{N_l} a^2)$ vs z/h of sandwich plates.

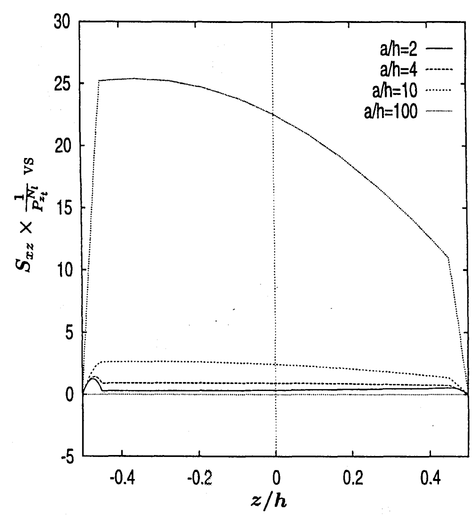

Fig. 12 Transverse shear stress $S_{xz} \times (1/P_{z_t}^{N_l})$ vs z/h of sandwich plates.

Conclusions

The numerical performances of LWM theories formulated on the basis of Reissner's mixed variational equations are discussed. Exact closed-form solutions, related to bending of symmetrically, asymmetrically laminated, and sandwich plates are considered. From a two-dimensional modeling point of view, the following points can be made.

1) With respect to existing theories, the proposed models permit one to completely and a priori fulfill the continuity conditions at the

interfaces for both displacement and transverse stress components (transverse displacement and transverse normal stress included).

2) The use of top and bottom values as unknown layer variables permits one easy linkage of the continuity conditions at a previous point by writing the governing equations from a layer to a multilayered level.

From the numerical analyses conducted, the following main conclusions can be made.

1) It has been confirmed that equivalent single-layer theories could be inadequate to evaluate transverse normal stress and the related effects of thick laminated plates. Furthermore, their accuracy depends very much on the anisotropy properties of the multilayered plates.

2) Mixed models lead to better description than standard displacement models. The related results match three-dimensional elasticity solutions very well. Furthermore, they lead to excellent a priori descriptions of transverse stresses, which means that such stresses can be evaluated without requiring any postprocessing procedures.

3) The accuracy of the present layerwise modelings has been confirmed for symmetrically and asymmetrically, as well as arbitrarily laminated, plates.

As the proposed models are of a two-dimensional type, they can be used instead of three-dimensional elasticity as reference solutions to assess simplified models. In fact, approximate solution procedures, e.g., finite elements, could be implemented to solve more complicated and general problems. In this respect, the computational costs could become prohibitive due to the dependence of the number of the unknowns on the number of layers. In such a case the use of a global–local approach would become imperative. These problems should be addressed by future investigations.

Appendix A: Arrays of Section II

The arrays in the mixed Hooke's law referred to a generic fiber orientation with respect to the x axis are

$$\boldsymbol{C}_{pp}^k = \begin{bmatrix} C_{11}^k & C_{12}^k & C_{16}^k \\ C_{12}^k & C_{22}^k & C_{26}^k \\ C_{16}^k & C_{26}^k & C_{66}^k \end{bmatrix}, \qquad \boldsymbol{C}_{pn}^k = \begin{bmatrix} 0 & 0 & C_{13}^k \\ 0 & 0 & C_{23}^k \\ 0 & 0 & C_{36}^k \end{bmatrix}$$

$$\boldsymbol{C}_{np}^k = \begin{bmatrix} 0 & 0 & 0 \\ 0 & 0 & 0 \\ -C_{13}^k & -C_{23}^k & -C_{36}^k \end{bmatrix}, \qquad \boldsymbol{C}_{nn}^k = \begin{bmatrix} C_{55}^k & -C_{45}^k & 0 \\ -C_{45}^k & C_{44}^k & 0 \\ 0 & 0 & C_{33}^k \end{bmatrix}$$

where

$$C_{ij}^k = \tilde{C}_{ij}^k - \frac{\tilde{C}_{i3}^k \tilde{C}_{3j}^k}{\tilde{C}_{33}^k}, \qquad i, j = 1, 2, 6$$

$$C_{i3}^k = \frac{\tilde{C}_{i3}^k}{\tilde{C}_{33}^k}, \qquad i = 1, 2, 6$$

$$C_{33}^k = \frac{1}{\tilde{C}_{33}^k}, \qquad C_{44}^k = \frac{\tilde{C}_{44}^k}{\Delta}, \qquad C_{55}^k = \frac{\tilde{C}_{55}^k}{\Delta},$$

$$C_{45}^k = \frac{\tilde{C}_{45}^k}{\Delta}, \qquad \Delta = \tilde{C}_{44}^k \tilde{C}_{55}^k - \tilde{C}_{45}^{k2}$$

The arrays of differential operators on Ω^k are

$$\boldsymbol{D}_p = \begin{bmatrix} \partial_x & 0 & 0 \\ 0 & \partial_y & 0 \\ \partial_y & \partial_x & 0 \end{bmatrix}, \qquad \boldsymbol{D}_n = \begin{bmatrix} \partial_z & 0 & \partial_x \\ 0 & \partial_z & \partial_y \\ 0 & 0 & \partial_z \end{bmatrix}$$

$$\boldsymbol{D}_{n\Omega} = \begin{bmatrix} 0 & 0 & \partial_x \\ 0 & 0 & \partial_y \\ 0 & 0 & 0 \end{bmatrix}, \qquad \boldsymbol{D}_{nz} = \begin{bmatrix} \partial_z & 0 & 0 \\ 0 & \partial_z & 0 \\ 0 & 0 & \partial_z \end{bmatrix}$$

The further arrays introduced at Eq. (13) are

$$\boldsymbol{I} = \begin{bmatrix} 1 & 0 & 0 \\ 0 & 1 & 0 \\ 0 & 0 & 1 \end{bmatrix}, \qquad \boldsymbol{I}_p = \begin{bmatrix} 1 & 0 & 0 \\ 0 & 1 & 0 \\ 1 & 1 & 0 \end{bmatrix}, \qquad \boldsymbol{I}_{n\Omega} = \begin{bmatrix} 0 & 0 & 1 \\ 0 & 0 & 1 \\ 0 & 0 & 0 \end{bmatrix}$$

Appendix B: Arrays at Equation (13)

The explicit forms of the differential operators related to displacement formulations are

$$\boldsymbol{K}_u^{k\tau s} = \begin{bmatrix} k_{xx} & k_{xy} & k_{xz} \\ k_{yx} & k_{yy} & k_{yz} \\ k_{zx} & k_{zy} & k_{zz} \end{bmatrix}, \qquad \boldsymbol{\Pi}_d^{k\tau s} = \begin{bmatrix} \pi_{xx} & \pi_{xy} & 0 \\ \pi_{yx} & \pi_{yy} & 0 \\ \pi_{zx} & \pi_{zy} & \pi_{zz} \end{bmatrix}$$

where

$$k_{xx} = E_{\tau_z s_z}^k \tilde{C}_{44} - E_{\tau s}^k \left(\tilde{C}_{11}^k \partial_{xx} + 2\tilde{C}_{16}^k (\partial_x \partial_y + \partial_y \partial_x) + \tilde{C}_{66}^k \partial_{yy}\right)$$

$$k_{xy} = k_{yx} = E_{\tau_z s_z} \tilde{C}_{45} - E_{\tau s}^k \left(\tilde{C}_{16}^k \partial_{xx} + \tilde{C}_{12}^k \partial_x \partial_y + C_{66}^k \partial_y \partial_x + \tilde{C}_{26}^k \partial_{yy}\right)$$

$$k_{xz} = -E_{\tau s_z} \left(\tilde{C}_{13}^k \partial_x + \tilde{C}_{36}^k \partial_y\right) + E_{\tau_z s} \left(\tilde{C}_{44}^k \partial_x + \tilde{C}_{45}^k \partial_y\right)$$

$$k_{yy} = E_{\tau_z s_z} \tilde{C}_{55} - E_{\tau s}^k \left(\tilde{C}_{22}^k \partial_{yy} + 2\tilde{C}_{26}^k (\partial_x \partial_y + \partial_y \partial_x) + \tilde{C}_{66}^k \partial_{xx}\right)$$

$$k_{yz} = -E_{\tau s_z} \left(\tilde{C}_{23}^k \partial_y + \tilde{C}_{36}^k \partial_x\right) + E_{\tau_z s} \left(\tilde{C}_{45}^k \partial_x + \tilde{C}_{55}^k \partial_y\right)$$

$$k_{zx} = E_{\tau_z s} \left(\tilde{C}_{13}^k \partial_x + \tilde{C}_{36}^k \partial_y\right) - E_{\tau s_z} \left(\tilde{C}_{44}^k \partial_x + \tilde{C}_{45}^k \partial_y\right)$$

$$k_{zy} = E_{\tau_z s} \left(\tilde{C}_{23}^k \partial_y + \tilde{C}_{36}^k \partial_x\right) - E_{\tau s_z} \left(\tilde{C}_{45}^k \partial_x + \tilde{C}_{55}^k \partial_y\right)$$

$$k_{zz} = E_{\tau_z s_z}^k \tilde{C}_{33} - E_{\tau s}^k \left(\tilde{C}_{44}^k \partial_{xx} + 2\tilde{C}_{45}^k (\partial_x \partial_y + \partial_y \partial_x) + \tilde{C}_{55}^k \partial_{yy}\right)$$

$$\pi_{xx} = E_{\tau s}^k \left(\tilde{C}_{11}^k + \tilde{C}_{16}^k\right) \partial_x + E_{\tau s}^k \left(\tilde{C}_{16}^k + \tilde{C}_{66}^k\right) \partial_y$$

$$\pi_{xy} = \pi_{yx} = E_{\tau s}^k \left(\tilde{C}_{16}^k + \tilde{C}_{66}^k\right) \partial_x + E_{\tau s}^k \left(\tilde{C}_{12}^k + \tilde{C}_{26}^k\right) \partial_y$$

$$\pi_{yy} = E_{\tau s}^k \left(\tilde{C}_{26}^k + \tilde{C}_{66}^k\right) \partial_x + E_{\tau s}^k \left(\tilde{C}_{22}^k + \tilde{C}_{26}^k\right) \partial_y$$

$$\pi_{zx} = E_{\tau s_z} \left(\tilde{C}_{44}^k + \tilde{C}_{45}^k\right), \qquad \pi_{zy} = E_{\tau s_z} \left(\tilde{C}_{45}^k + \tilde{C}_{55}^k\right)$$

$$\pi_{zz} = E_{\tau s}^k \left(\tilde{C}_{44}^k + \tilde{C}_{45}^k\right) \partial_x + E_{\tau s}^k \left(\tilde{C}_{45}^k + \tilde{C}_{55}^k\right) \partial_y$$

For the mixed case one has

$$\boldsymbol{K}_{uu}^{k\tau s} = -E_{\tau s}^k \begin{bmatrix} C_{11}^k \partial_{xx} + 2C_{16}^k (\partial_x \partial_y + \partial_y \partial_x) + C_{66}^k \partial_{yy} & C_{16}^k \partial_{xx} + C_{12}^k \partial_x \partial_y + C_{66}^k \partial_y \partial_x + C_{26}^k \partial_{yy} & 0 \\ \text{symmetric} & C_{22}^k \partial_{yy} + 2C_{26}^k (\partial_x \partial_y + \partial_y \partial_x) + C_{66}^k \partial_{xx} & 0 \\ & & 0 \end{bmatrix}$$

$$\boldsymbol{K}_{u\sigma}^{k\tau s} = \begin{bmatrix} E_{\tau_z s} & 0 & -E_{\tau s}^k \left(C_{13}^k \partial_x + C_{36}^k \partial_y\right) \\ 0 & E_{\tau_z s} & -E_{\tau s}^k \left(C_{36}^k \partial_x + C_{23}^k \partial_y\right) \\ -E_{\tau s}^k \partial_x & -E_{\tau s} \partial_y & E_{\tau_z s} \end{bmatrix}, \qquad \boldsymbol{K}_{\sigma u}^{k\tau s} = \begin{bmatrix} E_{\tau s_z} & 0 & E_{\tau s}^k \partial_x \\ 0 & E_{\tau s_z} & E_{\tau s}^k \partial_y \\ E_{\tau s}^k \left(C_{13}^k \partial_x + C_{36}^k \partial_y\right) & E_{\tau s}^k \left(C_{36}^k \partial_x + C_{23}^k \partial_y\right) & E_{\tau s_z} \end{bmatrix}$$

$$\boldsymbol{K}_{\sigma\sigma}^{k\tau s} = E_{\tau s}^k \begin{bmatrix} -C_{55}^k & C_{45}^k & 0 \\ C_{45}^k & -C_{44}^k & 0 \\ 0 & 0 & -C_{33}^k \end{bmatrix}, \qquad \boldsymbol{\Pi}_u^{k\tau s} = E_{\tau s}^k \begin{bmatrix} (C_{11}^k + C_{16}^k)\partial_x + (C_{16}^k + C_{66}^k)\partial_y & (C_{16}^k + C_{66}^k)\partial_x + (C_{12}^k + C_{26}^k)\partial_y & 0 \\ (C_{16}^k + C_{12}^k)\partial_x + (C_{26}^k + C_{66}^k)\partial_y & (C_{26}^k + C_{66}^k)\partial_x + (C_{22}^k + C_{26}^k)\partial_y & 0 \\ 0 & 0 & 0 \end{bmatrix}$$

$$\boldsymbol{\Pi}_u^{k\tau s} = E_{\tau s}^k \begin{bmatrix} 0 & 0 & C_{13}^k \\ 0 & 0 & C_{23}^k \\ 1 & 1 & C_{36}^k \end{bmatrix}$$

Appendix C: Integrals of Equation (14)

The integrals at Eqs. (14) related to a linear field in the k-layer written as arrays hold:

$$E^k_{\tau s} = h_k \begin{bmatrix} \frac{1}{3} & \frac{1}{6} \\ \frac{1}{6} & \frac{1}{3} \end{bmatrix}, \qquad E_{\tau_z s} = \begin{bmatrix} \frac{1}{2} & \frac{1}{2} \\ -\frac{1}{2} & -\frac{1}{2} \end{bmatrix}, \qquad E_{\tau s_z} = \begin{bmatrix} \frac{1}{2} & -\frac{1}{2} \\ \frac{1}{2} & -\frac{1}{2} \end{bmatrix}, \qquad E^k_{\tau_z s_z} = \frac{1}{h_k}\begin{bmatrix} 1 & -1 \\ -1 & 1 \end{bmatrix}$$

For the parabolic case they are

$$E^k_{\tau s} = h_k \begin{bmatrix} \frac{1}{3} & -\frac{1}{2} & \frac{1}{6} \\ -\frac{1}{2} & \frac{6}{5} & -\frac{1}{2} \\ \frac{1}{6} & -\frac{1}{2} & \frac{1}{3} \end{bmatrix}, \qquad E_{\tau_z s} = \begin{bmatrix} \frac{1}{2} & -1 & \frac{1}{2} \\ 1 & 0 & -1 \\ -\frac{1}{2} & 1 & -\frac{1}{2} \end{bmatrix}, \qquad E_{\tau s_z} = \begin{bmatrix} \frac{1}{2} & 1 & -\frac{1}{2} \\ -1 & 0 & 1 \\ \frac{1}{2} & -1 & -\frac{1}{2} \end{bmatrix}, \qquad E^k_{\tau_z s_z} = \frac{1}{h_k}\begin{bmatrix} 1 & 0 & -1 \\ 0 & 12 & 0 \\ -1 & 0 & 1 \end{bmatrix}$$

Appendix D: k-Layer Arrays Related to Navier-Type Solution

For the case of Navier-type solutions the preceding arrays take the following algebraic forms (the two parameters $\alpha = m\pi/a$ and $\beta = n\pi/b$ are introduced):

$$\hat{\boldsymbol{K}}^{k\tau s}_d = \begin{bmatrix} E^k_{\tau_z s_z}\tilde{C}_{44} + E^k_{\tau s}\left(\alpha^2\tilde{C}^k_{11} + \beta^2\tilde{C}^k_{66}\right) & E^k_{\tau s}\alpha\beta\left(\tilde{C}^k_{12} + \tilde{C}^k_{66}\right) & \alpha\left(-E_{\tau s_z}\tilde{C}^k_{13} + E_{\tau_z s}\tilde{C}^k_{44}\right) \\ E^k_{\tau s}\alpha\beta\left(\tilde{C}^k_{12} - C^k_{66}\right) & E^k_{\tau_z s_z}\tilde{C}_{55} + E_{\tau s}\left(\tilde{C}^k_{22}\beta^2 + \tilde{C}^k_{66}\alpha^2\right) & \beta\left(-E_{\tau s_z}\tilde{C}^k_{23} + E_{\tau_z s}\tilde{C}^k_{55}\right) \\ -\alpha\left(E_{\tau_z s}\tilde{C}^k_{13} - E_{\tau s_z}\tilde{C}^k_{44}\right) & -\beta\left(E_{\tau_z s}\tilde{C}^k_{23} - E_{\tau s_z}\tilde{C}^k_{55}\right. & E^k_{\tau_z s_z}\tilde{C}_{33} + E_{\tau s}\left(\alpha^2\tilde{C}^k_{44}\partial_{xx} + \beta^2\tilde{C}^k_{55}\right) \end{bmatrix}$$

$$\hat{\boldsymbol{\Pi}}^{k\tau s}_d = \begin{bmatrix} E^k_{\tau s}\left(-\tilde{C}^k_{11}\alpha + \tilde{C}^k_{66}\beta\right) & E^k_{\tau s}\left(\tilde{C}^k_{66}\alpha - \tilde{C}^k_{12}\beta\right) & 0 \\ E^k_{\tau s}\left(-\tilde{C}^k_{12}\alpha + \tilde{C}^k_{66}\beta\right) & E^k_{\tau s}\left(\tilde{C}^k_{66}\alpha - \tilde{C}^k_{22}\beta\right) & 0 \\ E_{\tau s_z}\tilde{C}^k_{44} & E_{\tau s_z}\tilde{C}^k_{55} & E^k_{\tau s}\left(\tilde{C}^k_{44}\alpha + \tilde{C}^k_{55}\beta\right) \end{bmatrix}, \qquad \hat{\boldsymbol{K}}^{k\tau s}_{uu} = -E^k_{\tau s}\begin{bmatrix} -C^k_{11}\alpha^2 - C^k_{66}\beta^2 & -C^k_{12}\alpha\beta - C^k_{66}\alpha\beta & 0 \\ \text{symmetric} & -C^k_{22}\beta^2 - C^k_{66}\alpha^2 & 0 \\ & & 0 \end{bmatrix}$$

$$\hat{\boldsymbol{K}}^{k\tau s}_{u\sigma} = \begin{bmatrix} E_{\tau_z s} & 0 & -E^k_{\tau s}C^k_{13}\alpha \\ 0 & E_{\tau_z s} & -E^k_{\tau s}C^k_{23}\beta \\ E^k_{\tau s}\alpha & E^k_{\tau s}\beta & E_{\tau_z s} \end{bmatrix}, \qquad \hat{\boldsymbol{K}}^{k\tau s}_{\sigma u} = \begin{bmatrix} E_{\tau s_z} & 0 & E^k_{\tau s}\alpha \\ 0 & E_{\tau s_z} & E^k_{\tau s}\beta \\ -E^k_{\tau s}C^k_{13}\alpha & -E^k_{\tau s}C^k_{23}\beta & E_{\tau s_z} \end{bmatrix}, \qquad \hat{\boldsymbol{K}}^{k\tau s}_{\sigma\sigma} = E^k_{\tau s}\begin{bmatrix} -C^k_{55} & C^k_{45} & 0 \\ C^k_{45} & -C^k_{44} & 0 \\ 0 & 0 & -C^k_{33} \end{bmatrix}$$

$$\hat{\boldsymbol{\Pi}}^{k\tau s}_u = E^k_{\tau s}\begin{bmatrix} -C^k_{11}\alpha + C^k_{66}\beta & C^k_{66}\alpha - C^k_{12}\beta & 0 \\ -C^k_{12}\alpha + C^k_{66}\beta & C^k_{66}\alpha - C^k_{22}\beta & 0 \\ 0 & 0 & 0 \end{bmatrix}, \qquad \hat{\boldsymbol{\Pi}}^{k\tau s}_u = E^k_{\tau s}\begin{bmatrix} 0 & 0 & C^k_{13} \\ 0 & 0 & C^k_{23} \\ 1 & 1 & 0 \end{bmatrix}$$

References

[1]Pagano, N. J., "Exact Solutions for Composite Laminates in Cylindrical Bending," *Journal of Composite Materials*, Vol. 3, July 1969, pp. 398–411.

[2]Srinivas, S., and Rao, A. K., "Bending, Vibration and Buckling of Simply Supported Thick Othotropic Rectangular Plates and Laminates," *International Journal of Solids and Structures*, Vol. 30, No. 11, 1970, pp. 495–507.

[3]Pagano, N. J., and Hatfield, C. J., "Elastic Behavior of Multilayered Bidirectional Composites," *AIAA Journal*, Vol. 10, No. 7, 1972, pp. 931–933.

[4]Carrera, E., "A Class of Two Dimensional Theories for Multilayered Plates Analysis," *Atti Accademia delle Scienze di Torino, Memorie Scienze Fisiche*, Vol. 19–20, Accademia delle Scienze di Torino, Turin, Italy, 1995–1996, pp. 49–87.

[5]Sun, C. T., and Whitney, J. M., "On the Theories for the Dynamic Response of Laminated Plates," *AIAA Journal*, Vol. 11, No. 2, 1973, pp. 372–398.

[6]Librescu, L., and Reddy, J. N., "A Critical Review and Generalization of Transverse Shear Deformable Anisotropic Plates," *Refined Dynamical Theories of Beams, Plates and Shells and Their Applications*, edited by I. Elishakoff and H. Irretier, Springer–Verlag, Berlin, 1987, pp. 32–43.

[7]Kapania, R. K., and Raciti, S., "Recent Advances in Analysis of Laminated Beams and Plates, Part I: Shear Effects and Buckling," *AIAA Journal*, Vol. 27, 1989, pp. 923–934.

[8]Noor, A. K., Burton, S., and Bert, C. W., "Computational Model for Sandwich Panels and Shells," *Applied Mechanics Review*, Vol. 49, 1996, pp. 155–199.

[9]Yang, P. C., Norris, C. H., and Stavsky, Y., "Elastic Wave Propagation in Heterogeneous Plates," *International Journal of Solids and Structures*, Vol. 2, 1966, pp. 85–97.

[10]Lo, K. H., Christensen, R. M., and Wu, E. M., "A Higher-Order Theory of Plate Deformation Part 2: Laminated Plates," *Journal of Applied Mechanics*, Vol. 44, 1977, pp. 669–676.

[11]Robbins, D. H., Jr., and Reddy, J. N., "Modeling of Thick Composites Using a Layer-Wise Theory," *International Journal of Numerical Methods in Engineering*, Vol. 36, 1993, pp. 655–677.

[12]Carrera, E., and Kröplin, B. H., "Zig-Zag and Interlaminar Equilibria Effects in Large Deflection and Postbuckling Analysis of Multilayered Plates," *Mechanics of Composite Material and Structures*, Vol. 4, 1997, pp. 89–94.

[13]Yu, Y.-Y., "A New Theory of Elastic Sandwich Plates. One Dimensional Case," *Journal of Applied Mechanics*, Vol. 37, 1959, pp. 1031–1036.

[14]Reddy, J. N., "A Simple Higher Order Theory for Laminated Composite Plates," *Journal of Applied Mechanics*, Vol. 51, No. 4, 1984, pp. 745–752.

[15]Cho, M., and Parmerter, R. R., "Efficient Higher Order Composite Plate Theory for General Lamination Configurations," *AIAA Journal*, Vol. 31, No. 7, 1993, pp. 1299–1305.

[16]Pei, C. C., and Corleone, J., "Transverse Shear in Laminated Plates Theories," *AIAA Journal*, Vol. 11, No. 9, 1973, pp. 1333–1336.

[17]Di Sciuva, M., Cicorello, A., and Dalle Mura, E., "A Class of Multilayered Anisotropic Plate Elements Including the Effects of Transverse Shear Deformability," Associazione Italiana di Aeronautica e Astronautica Conf., Turin, Italy, 1985, pp. 877–892.

[18]Bhashar, B., and Varadan, T. K., "Refinement of Higher-Order Laminated Plate Theories," *AIAA Journal*, Vol. 27, No. 12, 1989, pp. 1830, 1831.

[19]Ren, J. G., "A New Theory for Laminated Plates," *Composite Science Technology*, Vol. 26, 1986, pp. 225–239.

[20]Lekhnitskii, S. G., "Strength Calculation of Composite Beams," *Vestnik inzhen. i tekhnikov*, No. 9, 1935.

[21]Lekhnitskii, S. G., *Anisotropic Plates*, Gordon and Breach, New York, 1968.

[22]Carrera, E., "C^0_z-Requirements: Models for the Two-Dimensional Analysis of Multilayered Structures," *Composite Structures*, Vol. 37, 1997, pp. 373–383.

[23]Goldenvaizer, A. N., *Theory of Thin Elastic Shells*, International Series of Monographs in Aeronautics and Astronautics, Pergamon, New York, 1961.

[24]Cicala, P., *Systematic Approach to Linear Shell Theory*, Levrotto and Bella, Turin, Italy, 1965.

[25]Hodges, D. H., Lee, B. W., and Atilgan, A. R., "Application of the Variational-Asymptotic Method to Laminated Composite Plates," *AIAA Journal*, Vol. 31, 1993, pp. 1674–1683.

[26]Satyrin, V. G., and Hodges, D. H., "On Asymptotically Correct Linear Laminated Plate Theory," *International Journal of Solids and Structures*, Vol. 33, 1996, pp. 3649–3671.

[27]Srinivas, S., "A Refined Analysis of Composite Laminates," *Journal of Sound and Vibration*, Vol. 30, No. 4, 1973, pp. 495–507.

[28]Reddy, J. N., "A Generalization of Two-Dimensional Theories of Laminated Composite Plates," *Communications in Applied Numerical Methods*, Vol. 3, 1987, pp. 173–180.

[29]Gaudenzi, P., Barboni, R., and Mannini, A., "A Finite Element Evaluation of Single-Layer and Multi-Layer Theories for the Analysis of Laminated Plates," *Composite Structures*, Vol. 30, 1995, pp. 427–440.

[30]Reissner, E., "On a Certain Mixed Variational Theory and Proposed Applications," *International Journal of Numerical Methods in Engineering*, Vol. 20, 1984, pp. 1366–1368.

[31]Reissner, E., "On a Mixed Variational Theorem and on a Shear Deformable Plate Theory," *International Journal of Numerical Methods in Engineering*, Vol. 23, 1986, pp. 193–198.

[32]Murakami, H., "Laminated Composite Plate Theory with Improved In-Plane Response," *Journal of Applied Mechanics*, Vol. 53, No. 3, 1986, pp. 661–666.

[33]Toledano, A., and Murakami, H., "A Composite Plate Theory for Arbitrary Laminated Configurations," *Journal of Applied Mechanics*, Vol. 54, No. 4, 1987, pp. 181–189.

[34]Toledano, A., and Murakami, H., "A Higher-Order Laminated Plate Theory with Improved In-Plane Responses," *International Journal of Solids and Structures*, Vol. 23, 1987, pp. 111–131.

[35]Rao, K. M., and Meyer-Piening, H. R., "Analysis of Thick Laminated Anisotropic Composite Plates by the Finite Element Method," *Composite Structures*, Vol. 15, 1990, pp. 185–213.

[36]Carrera, E., "C^0 Reissner-Mindlin Multilayered Plate Elements Including Zig-Zag and Interlaminar Stresses Continuity," *International Journal of Numerical Methods in Engineering*, Vol. 39, 1996, pp. 1797–1820.

[37]Carrera, E., "Mixed Layer-Wise Models for Multilayered Plates Analyses," Dipartimento di Ingegneria Aeronautica e Spaziale, Turin Polytechnic Inst., Rept. 130/97, Turin, Italy, 1997.

[38]Jones, R. M., *Mechanics of Composite Materials*, McGraw–Hill, New York, 1975.

G. A. Kardomateas
Associate Editor